Polymer Bulletin (2021) 78:3327–3351
https://doi.org/10.1007/s00289-020-03256-7

ORIGINAL PAPER

Design, characterization and evaluation of cucurbitacin B-loaded core–shell-type hybrid nano-sized particles using DoE approach

Ceyda Tuba Sengel-Turk[1] · Nuri Ozmen[2] · Filiz Bakar-Ates[2]

Received: 4 November 2019 / Revised: 13 March 2020 / Accepted: 10 June 2020 /
Published online: 20 June 2020

Abstract

The main objective of this research was to design and optimize novel core–shell-type hybrid nano-sized systems of cucurbitacin B (CuB) based on the design of experiment (DoE) approach. The hybrid formulations consisting of polyethylene glycol (PEG)-conjugated phospholipid, lecithin and poly-lactic-co-glycolic acid (PLGA) were produced by employing self-assembly modified nanoprecipitation technique. A 3^2 factorial design was utilized to understand the effect of two input factors, namely PEG phospholipid/polymer ratio and total lipids/lecithin ratio, on entrapment efficiency and drug release percentage. The particle size and surface charge analyses, excipient interactions and thermal behavior, particle morphology, presence and thickness of lipid shell, and also storage stability studies were carried out through in vitro characterization. The entrapment efficiency of all nanoparticles of CuB ranged between 49.35 and 80.00%. The prepared lipid–polymer hybrid systems exhibited an average particle size from 94.5 to 127.2 nm with polydispersity in the range from 0.094 to 0.114, which inhibited a narrow size distribution. The nano-sized formulation at the center point of the design was selected as optimum formulation due to its excellent characteristics and the configuration determined using ANOVA and response surface methodology (RSM) approach.

Keywords Core–shell-type lipid polymer hybrid systems · Cucurbitacin B · Response surface methodology · 3^2 full factorial design

✉ Ceyda Tuba Sengel-Turk
ctsengel@pharmacy.ankara.edu.tr

[1] Department of Pharmaceutical Technology, Ankara University, Faculty of Pharmacy, 06100 Anadolu, Ankara, Turkey

[2] Department of Biochemistry, Ankara University, Faculty of Pharmacy, 06100 Anadolu, Ankara, Turkey

Introduction

Cucurbitacins are a class of tetracyclic triterpenoid molecules, extracted from the various plant families such as *Cucurbitaceae*, *Cruciferae*, *Rubiaceae*, *Scrophulariaceae*, *Primulaceae* and *Datiscaceae*. Among its derivates, cucurbitacin B (CuB) is a major active member of this family due to its wide range of biological activities such as antimicrobial, anti-inflammatory, antihelmenthic, antidiabetic, cardiovascular, hepatoprotective and hepatocurative effects [1, 2]. Additionally, the anticancer activity of the compound has also been demonstrated on various cancer cell lines through in vitro and in vivo experiments [3–5]. Although it is commercially available in a tablet form in China due to its widespread mechanism of action, its clinical use is limited due to its dose-dependent hematological toxicity, gastrointestinal side effects and low bioavailability because of its poor aqueous solubility and permeability characteristics [2, 6–8]. The main fundamental approach to provide and/or increase the clinical use of CuB is to overcome these limitations through the design of nano-sized drug delivery systems [9]. From this perspective, CuB-encapsulated solid lipid nanoparticles [10, 11], nanostructured lipid carriers [12], nanosuspensions [13], various micel formulation combinations [14–17], polymeric nanoparticles [7], nanoliposomes [18] and nanoemulsions [19, 20] have been developed by various researchers for this purpose.

Among the various types of nano-sized drug delivery strategies, polymeric and vesicular-type systems are the most researched and favored nano-sized carriers, as evidenced by numerous research reports, clinical trials and approved pharmaceutical products [2, 21–23]. Polymeric nanoparticles are spherical-shaped matrix-like structures, mostly composed of biodegradable polymers. The beginning of the active agent release from the carrier before arriving the target tissues, non-adaptable fabrication methods for industrial production, the excessive costs incurred and the requirement to use organic solvents in their production process are the major drawbacks that limit the use of polymeric nanoparticles as drug delivery systems [24–27]. On the other hand, liposomes are spherical-shaped vesicular structures in which an aqueous inner core is surrounded by single or multiple phospholipid double layers [18]. However, there are serious limitations for their clinical use due to their limited administration through the oral route, limited physical and chemical stability, short circulation half-life and also the storage shelf-life, low drug loading capacity and compatibility with industrial production scaling [28, 29]. The new generation of unique nano-sized carriers, named as lipid polymer hybrid systems, is an integrated design, which contribute to the structural superiorities of polymeric nanoparticles and liposomes by its own nature and thereby overcome limitations of both these carrier systems. These systems are core–shell-type hybrid nano-sized carriers that combine the mechanical superiorities of biodegradable polymer-based nanocarriers and the biomimetic benefits of liposomes within a stable carrier system [30–32]. These systems consist of three structural components: (1) a polymeric internal structure in which hydrophobic therapeutic agents have been entrapped; (2) a lipid layer surrounding the internal structure to prevent the leakage of the therapeutic active substance

from the internal structure and thereby acting as a biocompatible barrier; and (3) an outer lipid hydrophilic polymer stealth layer that serves to prolong the in vivo circulation half-life of the nanocarriers and also to enhance their physical and biological stability [31, 33, 34].

The main purpose of this study is to produce CuB-loaded lipid polymer hybrid nanoparticulate systems and to optimize the formulation variables affecting the basic particle characteristics such as entrapment efficiency and drug release. Factorial design is a statistical approach and conducts systematic scientific researches to determine the impact of the independent variables on the responses of the dependent variables. RSM is also performed by applying factorial design. The 3^2 factorial design consists of a center point for determining experimental reproducibility and nine design points for estimating linearity [35–37]. In this research, optimization of hybrid nanocarriers was carried out using the 3^2 factorial design through Design Expert 6.0.8 software. Two formulation parameters, PEG-conjugated phospholipid/biodegradable polymer ratio (*X1*) and the total lipids/lecithin molar percentage ratio (*X2*), were selected as independent variables. The response variables investigated to characterize the hybrid systems were the entrapment efficiency percentage ($Q1$) and drug release % at 24th h ($Q2$) of the hybrid nanoparticles. Moreover, excipient interactions and thermal behavior, particle morphology, presence and thickness of lipid shell, and storage stability characteristics of the optimized hybrid formulation were also evaluated in this context.

Materials and methods

Materials

The materials used were: CuB (TRC, Canada); 1,2-distearoyl-sn-glycero-3-phosphoetanolamine-N-carboxy(poly(ethylene glycol) (DSPE-PEG-COOH) 2000 (Avanti Polar Lipids, Alabaster, AL, USA); lecithin (Fluka, Germany); PLGA with a 50:50 monomer ratio (Sigma-Aldrich Chem. Co., Munich, Germany). All other chemicals used were at least of pharmaceutical grade.

Preparation of hybrid nanocarriers

A self-assembly modified nanoprecipitation method was utilized for the production of CuB-entrapped hybrid nano-sized carriers [31]. PLGA was used as a biodegradable polymeric core material, lecithin was selected as a lipid material, and DSPE-PEG-COOH 2000 was utilized as a PEG-conjugated phospholipid material. Stock solutions of lecithin and PEG-conjugated phospholipid were prepared separately in 4% aqueous ethanol solution at a concentration of 1 mg/mL. Stock acetonitrile solutions of polymer and CuB were also produced at a concentration of 2.5 mg/mL and 15% by weight polymer, respectively. The calculated amounts of lecithin and PEG-conjugated phospholipid solutions for each formulation group were added to the distilled water and sonicated (Jeio Tech US-05, Jeio Tech, Co. Ltd., Korea). The

polymer and CuB mixture were added to the lipid phase, and the resulting dispersion was sonicated for 7 min at 40 kHz ultrasonic power at 35 °C in an ultrasonic bath. In all formulations, the dispersion volume was adjusted to 8 ml with distilled water so that the organic/aqueous phase volume ratio was 1:10. The concentrated hybrid nanoparticles were obtained by using Vivaspin 20 centrifuge filter. Lyophilization process was carried out for 2 days to obtain solid nanoparticles (Christ Gamma 2-16 LSC, Martin Christ Gef., Germany). The PEG-conjugated phospholipid amount varied from 200 to 400 and 800 µg to obtain *X1* values of 0.1, 0.2 and 0.4 while keeping the polymer amount constant at 2000 µg. 17%, 34% and 68% molar ratios were selected as *X2* values to create 3^2 factorial design combinations based on DoE approach (Tables 1, 2).

Characterization of hybrid nanocarriers

Entrapment efficiency

Content of the CuB in the hybrid nano-sized particles was determined through a high-performance liquid chromatography (HPLC) method developed by Sturm and Stuppner [38] and Bajcsik et al. [39]. This developed method was modified for hybrid nano-sized systems and then used for the detection. The HPLC analysis was

Table 1 Content of the CuB-loaded hybrid nanoparticles

Code	Content of the hybrid formulations						
	Organic phase			Aqueous lipid phase			
	PLGA (µg)	CuB (µg)	Acetonitrile (µL)	DSPE-PEG (µg)	Lecithin (µg)	Ethanol solution (4%, µL)	Enough amount of water (µL)
Design point formulations							
LP1	2000	300	800	200	5	205	8000
LP2	2000	300	800	200	12	212	8000
LP3	2000	300	800	200	50	250	8000
LP4	2000	300	800	400	10	410	8000
LP5	2000	300	800	400	25	425	8000
LP6	2000	300	800	400	100	500	8000
LP7	2000	300	800	800	20	820	8000
LP8	2000	300	800	800	48	848	8000
LP9	2000	300	800	800	200	1000	8000
Center point formulations							
LP10	2000	300	800	400	25	425	8000
LP11	2000	300	800	400	25	425	8000
LP12	2000	300	800	400	25	425	8000
LP13	2000	300	800	400	25	425	8000

Table 2 Full factorial design of two independent factors at three levels and entrapment efficiency percentage (*Q1*) and drug release percentage at 24th h (*Q2*) as response variables

Formulation code	Variable coded levels		Actual variables		Response variables			
	PEG-conjugated phospholipid/biodegradable polymer ratio (*X1*)	Total lipids/lecithin molar percentage ratio (*X2*)	PEG-conjugated phospholipid/biodegradable polymer ratio (*X1*)	Total lipids/lecithin molar percentage ratio (*X2*) (%)	Observed variables		Predicted variables through DoE	
					Entrapment efficiency (% ± SD) (*Q1*)	Drug release at 24th h (% ± SD) (*Q2*)	Entrapment efficiency (%) (*Q1*)	Drug release at 24th h (%) (*Q2*)
Design points								
LP1	−1	−1	0.1	17	49.35 ± 8.52	28.68 ± 1.17	48.18	28.17
LP2	−1	0	0.1	34	54.25 ± 1.33	29.68 ± 1.45	58.94	30.72
LP3	−1	+1	0.1	68	61.33 ± 6.58	28.44 ± 1.03	57.81	27.91
LP4	0	−1	0.2	17	64.60 ± 6.63	16.80 ± 0.03	65.87	17.68
LP5	0	0	0.2	34	80.00 ± 4.97	20.01 ± 0.02	76.66	20.03
LP6	0	+1	0.2	68	69.59 ± 8.31	16.08 ± 1.01	75.56	17.02
LP7	+1	−1	0.4	17	55.97 ± 8.55	10.08 ± 1.14	55.87	9.71
LP8	+1	0	0.4	34	64.13 ± 0.42	11.08 ± 1.02	66.68	11.86
LP9	+1	+1	0.4	68	68.06 ± 7.56	9.05 ± 1.33	65.61	8.65
Center points								
LP10	0	0	0.2	34	78.03 ± 1.57	20.61 ± 0.07	76.66	20.03
LP11	0	0	0.2	34	77.60 ± 2.56	20.28 ± 0.12	76.66	20.03
LP12	0	0	0.2	34	77.28 ± 3.44	20.50 ± 0.23	76.66	20.03
LP13	0	0	0.2	34	77.62 ± 4.93	20.58 ± 0.41	76.66	20.03

Coded levels	Actual values	
	X1	*X2* (%)
+1	0.4	68
0	0.2	34
−1	0.1	17

carried out by the Agilent 1100 series LC system (USA) equipped with diode array detector. ACE C18 (150 mm × 4.6 mm; 5 µm) column was used for the sample separation. The column was preconditioned for about 30 min before the first injection. The mobile phase consisting of a mixture of acetonitrile–water (70:30;v/v) which contains trifluoroacetic acid (0.1%) was used for separation and analysis of CuB. Prepared mobile phase was degassed in an ultrasonic bath for 15 min. The flow rate was maintained at 1 mL/min. The chromatographic conditions were as follows: volume injected 20 µL, detection wavelength of CuB at 248 nm. To determine the amount of CuB-entrapped on the hybrid nanoparticles, the free amount of CuB in the supernatant was analyzed through HPLC. The entrapment efficiency percentage of CuB was calculated using the following equation [40]:

$$\text{Entrapment efficiency } \% = \left[\left(\text{Weight}_{\text{total CuB}} - \text{Weight}_{\text{free CuB}}\right)/\text{Weight}_{\text{total CuB}}\right] \times 100$$

$$\text{Weight}_{\text{total CuB}} = \text{The total amount of CuB}$$

$$\text{Weight}_{\text{free CuB}} = \text{The amount of CuB in the supernatant}$$

Analytical validation of the modified HPLC method was interpreted according to the ICH Q2 (R1) guideline criteria with respect to linearity and range, precision (inter-day and intraday precision), accuracy and recovery, specificity, and detection/quantitation limits that were analyzed.

Particle size and surface charge

Photon correlation spectroscopy (PCS) (Nano ZS, Malvern Inst., Malvern, Worcestershire, UK) was utilized for the determination of the mean particle size and size distribution (PDI) of the hybrid nano-sized particles. Zeta potential values of the particles were detected through Laser Doppler Anemometry (Malvern Nano ZS, Malvern Inst., Malvern, Worcestershire, UK). For measurements, the lyophilized hybrid nanoparticles were suspended in distilled water at a ratio of 1/10 (v/v). Mean values were calculated through three successive measurements for each system.

Transmission electron microscopy

The hybrid nano-sized particles were monitorized by using a Fei Tecnai G2 Spirit BioTWIN transmission electron microscope (TEM) (FEI Co., USA). Staining of the hybrid dispersions was carried out using 2% (w/v) uranyl acetate solution, and then the nanoparticles were taken up on a carbon-coated copper grid (AGAR Scientific, UK). Fixation was carried out at room temperature [41].

Solubility and in vitro drug release

Solubility and in vitro release performance of the CuB-entrapped hybrid nanocarriers were carried out in PBS pH 7.4. To maintain sink conditions during in vitro dissolution studies of CuB from lipid–polymer hybrid systems, the solubility property

of CuB was determined at the first stage. Excess amounts of bulk CuB were stirred in 50 ml PBS pH 7.4 on a multi-stirrer at a temperature of 37 ± 0.5 °C for a suitable time in order to achieve equilibrium. The samples were filtered using a 0.45-mm Sartorius filter, and the concentration of CuB into the filtrate was analyzed through HPLC method to define its solubility characteristics in the PBS pH 7.4 ($n = 3$). Once the sink conditions were obtained, in vitro CuB release studies of hybrid nano-sized particles were performed through utilizing dialysis bag method [27, 42]. A cellulose acetate dialysis bag (MWCO: 12–14 kDa) (Sigma-Aldrich) and phosphate buffer saline (PBS) pH 7.4 were utilized as the dialysis membrane and dissolution medium, respectively. Dispersed form of hybrid nanoparticles was placed into dialysis bags and then sop in 100 mL PBS under sink conditions ($n = 3$). An incubator which was set at 50 rpm and 37 °C was utilized for the incubation of the formulations (Jeio Tech SI-300, Jeio Tech Co. Ltd., Korea). At predetermined time intervals, a known amount of dissolution medium was withdrawn and then analyzed through HPLC [43].

Studies of thermal analysis

Thermal analysis of pure CuB, optimum hybrid system and the blank form of this optimized formulation were carried out by a differential scanning calorimeter (DSC) (DSC 60, Shimadzu, Japan). Each lyophilized powder sample was weighed approximately the same amount and filled into aluminum pans. The analysis was performed by a scan between 25 and 250 °C with a heating rate of 5 °C per minute [44].

Small-angle X-ray scattering (SAXS) analysis

SAXS analysis was performed to determine the presence and also the thickness of lipid transition layer onto the surface of the optimum lipid–polymer hybrid systems. This transition layer was created through the lipid layer due to the electron density difference between the polymeric particles and the lipids. The thicknesses of the particles' lipid shells were measured using the Rigaku SmartLab X-Ray system with a 35 kW X-ray source (Rigaku, Japan). Measurements were utilized between 0.04 and 0.550 Å.

X-ray photoelectron spectroscopy (XPS) analysis

The presence of the lipid shell layer of the optimum hybrid nano-sized particles was confirmed through the XPS analysis. For this purpose, X-ray photoelectron spectrometer (PHI-5000 Versaprobe, Ulvac Physical Electronics, Japan) with a monochromated Al Kα source was utilized. Sensitivity and sufficient resolution were provided by fixation of the pass energy at 20 eV or 100 eV. Binding energies of the elements (eV) on the surface of the particles were obtained through the curve-fitting program XPSPEAK 4.1.

Storage stability

Storage stability of the optimum hybrid nano-sized particles at two different climatic conditions of 4 °C and 25 °C/60% relative humidity (RH) was evaluated over 3- and 6-month periods in terms of the entrapment efficiency, particle size, PDI and zeta potential characteristics.

Optimization by 3^2 factorial design

Multiple linear regression (MLR) analysis was performed to investigate the factors affecting the final properties of hybrid nanoparticles [34]. Nine hybrid nanoparticle formulations were prepared as per 3^2 factorial design to determine the impact of two input factors: PEG-conjugated phospholipid/biodegradable polymer ratio ($X1$) and the total lipids/lecithin molar percentage ratio ($X2$), on the two responses: entrapment efficiency percentage ($Q1$) and drug release % at 24th h ($Q2$) of the CuB-loaded hybrid nanoparticles. Three levels (− 1, 0 and 1) were selected for the testing of each factor. The regression equation of the fitted model for the responses was calculated using the following equation:

$$Q = b_o + b_1X1 + b_2X2 + b_3X1^2 + b_4X2^2 + b_5X1X2$$

To evaluate the response of variables in terms of interactive and polynomial terms, a statistical model was employed. In the model, Q is the independent variable; b_o is the arithmetic average response of nine experiments, and b_1, b_2, b_3, b_4 and b_5 were the forecasted coefficient for the factor $X1$ and $X2$. When two factors were changed at the same time, the term that indicates how the response changes was the interaction term ($X1X2$). Nonlinearity was investigated through the polynomial terms ($X1^2$ and $X2^2$). The results from factorial design were evaluated statistically through analysis of variance (ANOVA) test [31]. The values and the levels of factors investigated in this research and the variable levels are displayed in Table 2.

Results and discussion

Validation of analytical method

The analytical validation parameters of the modified HPLC method utilized for the determination of the amount of CuB loaded into the hybrid nano-sized particles were analyzed, and among them, the retention time of CuB was detected as 2.44 min. According to the validation data, the R^2 value of the method obtained at the concentration range between 5 and 400 µM was determined as 0.9999. The slope and the intercept of the calibration curve were calculated as 5.9708 and − 5.6519, respectively. By the obtained high R^2 value, the linearity of the response was confirmed. The low values of relative standard deviations of the inter-day (0.18%) and intraday (0.34%) precisions and also the standard errors of intercept (0.2409) and slope (0.0086) established the

precision of the modified HPLC method. The obtained LOD and LOQ values were calculated as 0.074 µg/mL and 0.225 µg/mL, respectively. Besides, the specificity of the HPLC method was achieved since the drug quantification did not interact with any of the ingredients used in the formulations. The analytical validation results demonstrated that the modified HPLC method was successfully applied for CuB analysis from the hybrid nano-sized systems.

Full factorial experimental design

The design and production of lipid–polymer hybrid nanoparticles are a highly complex process because it depends on many formulations and process parameters. These factors affect the final product characteristics significantly by displaying different interactions among each other. In our research, the main features defined for the developed nanoparticles are excellent shell–core structure, high encapsulation efficiency and the proper drug release rate. Considering the various studies in the area of hybrid carrier nanoscale systems, types of the PEG-conjugated lipids and polymers and also the molar lipid ratios are the most critical factors in providing the determined characteristics [30–34]. From this perspective, two FDA-approved excipients, PLGA and DSPE-PEG, were chosen as a hydrophobic polymeric core structure and a PEG-conjugated stealth shell former, respectively. Lecithin, a natural lipid, has been used as a lipid-structured monolayer between the interface of the polymeric core and the phospholipid shell. A 3^2 factorial design model was used in order to determine the influences of PEG-conjugated phospholipid/biodegradable polymer ratio and total lipids/lecithin molar ratios on the determined key properties of CuB-encapsulated hybrid nanoparticles. Table 1 shows the content of CuB-encapsulated hybrid nanoparticles based on the 3^2 full factorial design approach. The full factorial design types of optimization approaches and the applied computer programs create mathematical equation models for each response in order to determine the effectiveness of the input factors examined on the output variables and interpret the regression equations of the fitted models [34, 36]. The answer to the mathematical model developed in this way is also evaluated statistically. The levels of independent factors and response variables obtained in this research are displayed in Table 2. ANOVA was applied to determine the influence of each independent variable on the entrapment efficiency percentage (*Q1*) and drug release percentage at 24th h (*Q2*) and also indicate the fitness of the factorial design models. The data obtained as a result of the experimental design were placed in various design models such as 2FI (two-factor interaction), linear, quadratic and cubic models, and finally, the best design model which defines the correlation between the independent and the response variables was selected according to the highest coefficient of determination and F value of the model and also a statistically significant p value which was calculated based on the sum of squares analysis.

The effect of the factorial design on entrapment efficiency

One of the most important features of the hybrid nanoparticle formulations is the drug entrapment efficiency. The entrapment efficiency values of the CuB-loaded

hybrid systems prepared for this research were ranged between 49.35 and 80.00%, as given in Table 2. The response *Q1* values of the design were examined on the basis of input factors, PEG-conjugated phospholipid/biodegradable polymer ratio (*X1*) and total lipids/lecithin molar percentage ratio (*X2*). It was determined that the entrapment efficiency of hybrid nanoparticles increased in correlation with the increase in molar percentage ratio of total lipids/lecithin at the full levels of *X1* (Table 2). In accordance with the increase in *X2* levels, a greater amount of CuB could be incorporated into the polymeric core of hybrid nanoparticles due to the rise at the total lipid amounts in the lipid phase of the dispersion during production process. The main reason of this situation is the increase in the lipid shell layer thickness due to the increase in the *X2* level. Thus and so, the leakage of the high hydrophobic CuB from the polymeric core in the aqueous phase to the lipid phase during the formation of the hybrid nanoparticles was reduced[31]. When the *X1* ratio increased from −1.00 level to 0.00 level, the *Q1* response variable was positively affected and the highest *Q1* response value was used in the LP5-coded formulation on the center point of the design. In contrast, when the *X1* ratio increased from 0.00 level to +1.00 level, the response values of the *Q1* variable reduced significantly depending on the particle shape deformity due to the increase in the lipid amounts in the aqueous lipid phase of the dispersion during production process.

The ANOVA results given in Table 3 show that the factorial design developed in this research is fitted to the quadratic model with a significant p value ($p=0.0010$) and an insignificant lack of fit value ($p=0.5133$). Both the independent variables, *X1* and *X2*, have statistically significant influences on response variable *Q1* (Table 3). When the level of relationship between independent variables (*X1X2*) were examined, a non-interactive relation has been acquired ($p=0.9888$). The negative or positive signs in front of the coefficients of the input factors refer to the antagonistic or synergistic efficiencies of each input variable on each response variable[32]. From this point of view, it was seen that both *X1* and *X2* have a positive effect on the *Q1* response variable according to the regression equation given in Table 3. The model *F* value is an indicator of conformity to the mathematical equation model developed in the design, and it is interpreted in comparison with the tabulated F value [37]. In our research, the *F* value of the model developed for *Q1* response variable ($F=16.22$, Table 3) was obtained higher than tabulated *F* value ($F\text{tab}=4.46$), which indicates the significant difference of the developed model ($p=0.0010$). In a regression analysis, the coefficient of determination (R^2) is the value that shows how much of the dependent variable is expressed by the explanatory variables in that analysis [35]. The R^2 value of the model developed for the *Q1* response variable was calculated as 0.9205 (Table 3). The proximity of R^2 to 1 is an indicator of the convenience and accuracy of the developed model.

In addition to the design of the experiments within the scope of 3^2 factorial design, response surface methodology (RSM) approach is an assessment used to determine the optimum formulation. The RSM approach visually presents the visual effects of changes in a variable on the physicochemical parameters of the prepared nanoparticle formulations and helps to understand the effectiveness of input factors on output variables. Besides RSM approach, linearity graphics are also utilized to show compliance to the fitted model. The linearity plots give a

diagrammatical demonstration of the relationship between actual and predicted values of the responses [37]. The influence of independent factors on *Q1* response variable is demonstrated in Fig. 1a, b. It was shown that the highest entrapment efficiency of hybrid nanocarriers of about 80% occurs when the *X1* independent variable is between 0.00 level and + 1.00 level, and the *X2* variable is ranged from 0.00 level to + 0.50 level (Fig. 1a). In addition to the RSM graphics, the linearity plot of *Q1* was also demonstrated that the predicted values were close to the actual ones. As shown in the linearity plot of *Q1*, the linear existence of the plot was an indication of the linear relationship between *X1* and *X2* independent variables (Fig. 1c). LP5-coded hybrid systems with a combination of medium level of DSPE-PEG/PLGA ratio (*X1*) and total lipid/lecithin molar percentage ratio (*X2*) had the highest entrapment efficiency.

The effect of the factorial design on drug release

Solubility studies of CuB into the PBS pH 7.4 medium were performed to ensure the existence of the sink conditions during the in vitro drug release studies. This study notified that CuB was freely soluble in this medium. The solubility value of CuB was found to be 0.49 ± 0.02 mg/mL at the end of this analysis. Dissolution rate graphics expressing the amount of the drug released over time provide a preliminary information about the cell culture experiments and cytotoxicity profiles of the nanoparticles. In this respect, the percentage of drug release from the hybrid nano-sized particles at 24th h was chosen as another important response variable identified within the full factorial design. The release percentages of CuB from the hybrid systems at the end of 24th h are demonstrated in Table 2.

The CuB release from the hybrid formulations prepared at all design points ranged from 9.05 to 29.68% at 24th h. When the behavior of the *Q2* response variable was evaluated in terms of the effects of the *X1* and *X2* input factors, it was shown that all the levels of *X1* significantly affected the *Q2* response values ($p < 0.0001$, Table 3), whereas *X2* input factor had not a strong effect on the *Q2* output variable ($p = 0.3733$), as shown in the ANOVA results presented in Table 3. However, when the level of relationship between input variables (*X1X2*) was evaluated, it was found that there was a non-interactive relationship between two independent factors ($p = 0.6578$, Table 3). When the effects of the PEG-conjugated phospholipid/biodegradable polymer ratio (*X1*) were evaluated on *Q2* response values of hybrid nanocarriers, it was indicated that the rate of CuB release from the nanoparticle formulations at the end of the 24th h decreased significantly due to the increase in PEG-conjugated phospholipid amount compared to the polymer amount in the formulation content.

Regression equations of fitted model for *Q*1 and *Q*2

$$Q1 = 76.66 + 3.87X1 + 4.84X2 - 13.85X1^2 - 5.94X2^2 + 0.03X1.X2$$

$$Q2 = 20.03 + 9.43X1 - 0.33X2 + 1.26X1^2 - 2.68X2^2 + 0.20X1.X2$$

Table 3 ANOVA results for quadratic model to estimate all the response variables with 32 full factorial design

Responses	Source	Sum of squares	*df*	Mean square	*F* value	*p* value Prob > *F*		R^2	Adj R^2	Predicted R^2	Adeq precision
Q1	Model	1166.89	5	233.38	16.22	0.0010	Significant	0.9205	0.8638	0.4254	11.049
	X1	89.94	1	89.94	6.25	0.0410					
	X2	140.75	1	140.75	9.78	0.0167					
	$X1^2$	529.62	1	529.62	36.80	0.0005					
	$X2^2$	97.54	1	97.54	6.78	0.0353					
	X1X2	0.003	1	0.003	0.0002	0.9888					
	Residual	100.75	7								
	Lack of fit	95.98	3	31.99	26.84	0.5133	Not significant				
	Pure error	4.77	4	1.19							
	Cor total	1267.64	12								
Q2	Model	554.60	5	110.92	151.99	< 0.0001	Significant	0.9909	0.9844	0.9399	38.036
	X1	533.74	1	533.74	731.36	< 0.0001					
	X2	0.66	1	0.66	0.90	0.3733					
	$X1^2$	4.37	1	4.37	5.99	0.0443					
	$X2^2$	19.87	1	19.87	27.23	0.0012					
	X1X2	0.16	1	0.16	0.21	0.6578					
	Residual	5.11	7	0.73							
	Lack of fit	4.86	3	1.63	25.60	0.7045	Not significant				
	Pure error	0.25	4	0.063							
	Cor total	559.71	12								

When the level of *X1* increased, the thickness of the lipid shell also increased, and as a result, the percentage of CuB which released from the thickened lipid shell per unit time has decreased. As shown in Table 3, the highest fit for the *Q2* response variable was determined as the quadratic model (F value = 151.99, $p < 0.0001$). The R^2 value of the model was determined as 0.9909, which proved good and significant fit to the model (Table 3). The highest CuB release from the hybrid systems was obtained from the + 1.00 level to the − 1.00 level for *X1* according to the RSM graphics shown in Fig. 2a, b. This situation was arisen from the increase in the hydrophobic structure of the hybrid nano-sized particles due to the increase in the thickness of the lipid monolayer at the interface of the hydrophilic PEG-conjugated phospholipid shell and the hydrophobic polymeric core [32]. When the linearity graphic that belonged to *Q2* was examined, it was shown that the plot was found to be linear, demonstrating a linear relationship between *X1* and *X2* (Fig. 2c).

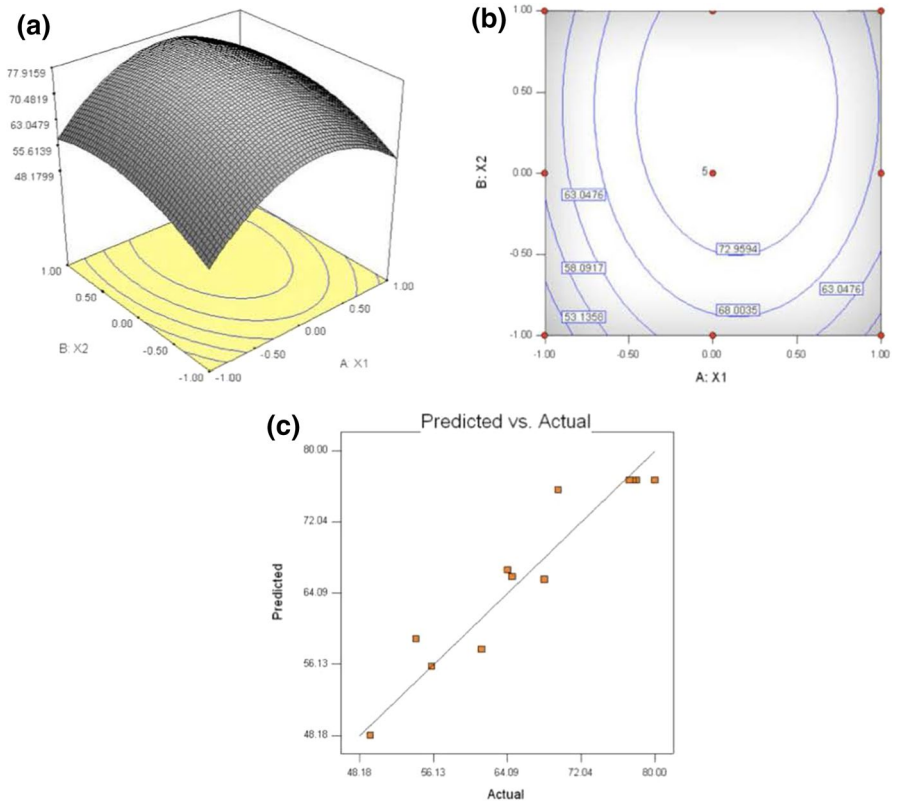

Fig. 1 **a** The response surface graphic, **b** the contour plot, and **c** the linearity graphic of hybrid nanoparticles demonstrating the influence of PEG-conjugated phospholipid/biodegradable polymer ratio (*X1*) and total lipids/lecithin molar percentage ratio (*X2*) on the entrapment efficiency (*Q1*) response

The adjusted (Adj) R^2 value indicates the generalizability of the model to which design fits. In other words, if the model was derived from the population instead of the sample, it would explain the total variance at the Adj R^2 level [45]. In this research, for both *Q1* and *Q2* response variables, the model R^2 values were found to be higher than the Adj R^2 values. Lower Adj R^2 values obtained from both output variables indicated that there was a significant relationship reflected through the model (Table 3).

In statistical modeling, signal-to-noise ratio is measured through adequate precision (AdeqPresicion) value. An AdeqPresicion value greater than 4 indicates that the proposed model is appropriate for the design space [46]. In this study, the AdeqPrecision values were found to be 11.049 and for the *Q1* response variable and 38.036 for the *Q2* response variable, which indicated an acceptable signal-to-noise ratio (Table 3).

The predicted R^2 value shows the closeness between the predicted results of the model and the actual results of the universe [34]. Predicted R^2 values of *Q1* and *Q2* response variables were 0.4254, and 0.9399, respectively (Table 3). The highest predicted R^2 value of *Q2* indicated an excellent fit to the model. This result correlated with both the highest F and the model R^2 values of *Q2* response variable ($p < 0.0001$).

Particle size and PDI of the hybrid nano-sized particles

The mean particle size of CuB-encapsulated hybrid nanocarriers ranged from 94.5 to 127.2 nm with PDI values between 0.094 and 0.122. The graphic of the particle sizes of the nano-sized hybrid carriers presented in Fig. 3 showed that the decrease at the investigated PEG-conjugated phospholipid/biodegradable polymer ratios and the total lipids/lecithin molar percentage ratios were in consistency with the reduction in the size of the particles due to the decrease in the lipid ratio in the hybrid formulation content ($p < 0.05$, Fig. 3a). The final viscosity of the dispersion was reduced with the reduction in the total amount of lipid present in the lipid phase during the production process, and consequently, the particle sizes of the hybrid systems were decreased [47]. The particle size distribution of the formulations prepared in nanoparticulate systems is expressed by the polydispersity index value. The polydispersity index is defined by the lognormal distribution width of the particle diameter. According to many researchers, the PDI value should be less than 0.2 for a homogeneous particle size distribution [24, 34]. When the developed CuB-encapsulated lipid polymer hybrid nanoparticle formulations were evaluated in terms of PDI values, it was observed that all obtained hybrid systems demonstrated a monodisperse structure (PDI value < 0.2, Fig. 3b).

Zeta potential of the hybrid nano-sized particles

Zeta potential is an important characterization parameter in terms of stability of a colloidal system, interaction of nanoparticles with cell membranes and their

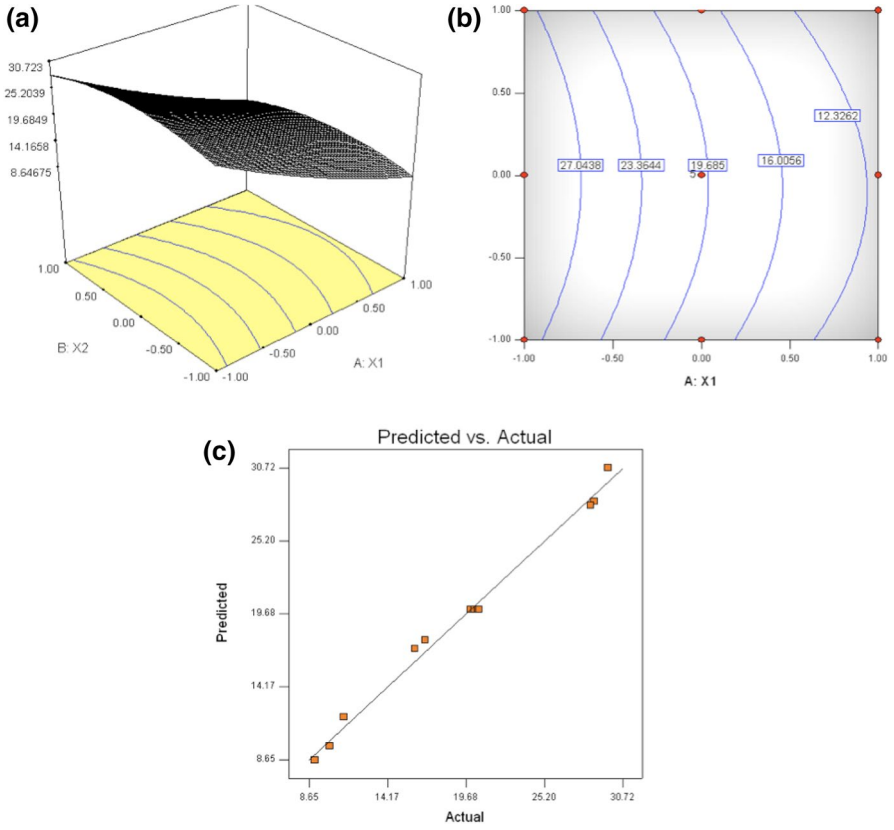

Fig. 2 **a** The response surface graphic, **b** the contour plot, and **c** the linearity graphic of hybrid nanoparticles demonstrating the influence of PEG-conjugated phospholipid/biodegradable polymer ratio (*X1*) and total lipids/lecithin molar percentage ratio (*X2*) on drug release percentage at 24th h (*Q2*)

biological activities. Appropriate high levels of zeta potential, either negative or positive, provide strong repulsion forces among the nanoparticles and thereby prevent agglomeration of the particles [10, 11, 13]. The lipid polymer hybrid nanocarriers of CuB had negative surface charges ranging from −29.60 to −40.50 mV as shown in Fig. 3c. The negative surface charge of the hybrid systems results from the presence of the phospholipid shell on the outer surface of the nanoparticle. A statistically significant increase was observed in the surface charges of the nanoparticles due to the increase in lipid content in all investigated DSPE-PEG/polymer ratios (0.1, 0.2 and 0.4) ($p < 0.05$). On the other hand, in terms of total lipid/lecithin molar percentage ratio (17%, 34% and 68%) which is named as *X2* independent variable, no statistically significant change was observed in the surface charge values of hybrid nanocarriers ($p > 0.05$).

TEM analysis of the hybrid nano-sized particles

The shape of the CuB-encapsulated hybrid nano-sized systems was visualized through TEM analysis as indicated in Fig. 4. Images of hybrid nano-sized particles reveal the effect of output factors on the structure properties of the hybrid systems. When the *X1* ratio is 0.1 or 0.2, the hybrid nanoparticles appear to have a spherical structure and homogeneous distribution with a light-colored internal polymeric core surrounded by a dark lipid layer [31, 32, 48]. The core–shell structure could be observed quite clearly in this formulation groups. On the other hand, as the *X1* ratio was risen to 0.4, the sphericity of the nanoparticles deteriorated due to the highest phospholipid content of this hybrid particle group. According to TEM images, when the *X1* ratio was 0.1 or 0.2, the nanoparticles showed no tendency to agglomerate. This is thought to result from sufficient repulsion forces among the nano-sized particles depending on the lipid content at the appropriate ratio. Among the examined input factors, *X1* variable has major effect compared to *X2* factor on the formation of spherical form and the core–shell structure of hybrid particles.

Optimization of the hybrid nano-sized particles

Optimum hybrid formulation was determined by using DoE approach based on *Q1* and *Q2* response variables. The overlaid contour plots for the CuB-entrapped hybrid nano-sized carriers are demonstrated in Fig. 5. The yellow area in the plots indicates where the critical desired outcomes are present, i.e., an entrapment efficiency percentage above or equal to 80%, a drug release percentage at 24th h approximately between 20 and 25% in consistency with our prior knowledge.

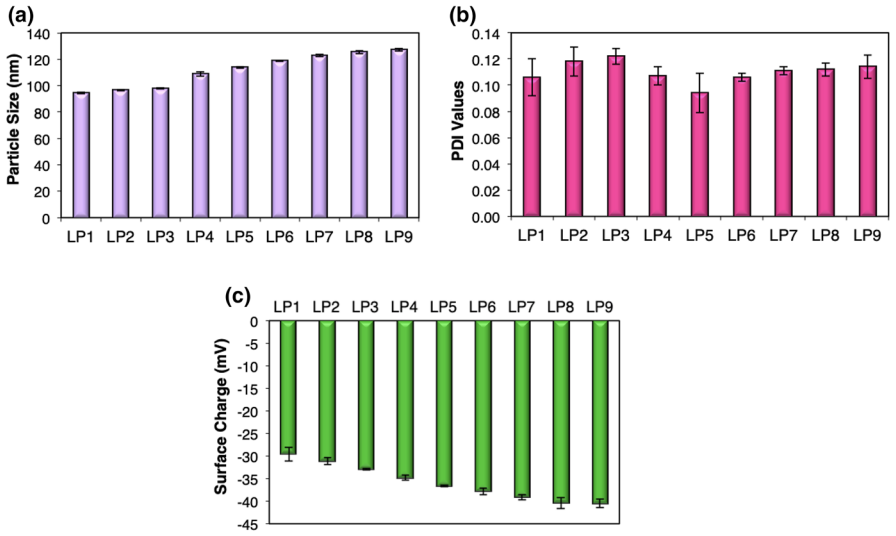

Fig. 3 **a** Particle size, **b** PDI and **c** zeta potential values of the CuB-encapsulated hybrid nano-sized particles

Once the overlaid contour plots were established, a desirable function (*d*) method was used to determine the optimum hybrid formulation of CuB having the targeted entrapment efficiency and drug release at 24th h [45, 49, 50]. A "*d*" value close to "1" states that the target outcomes are approached, while the "*d*" value close to zero indicates that desired response value has been moved away. For this purpose, the target variables need to be defined exactly. For this reason, the entrapment efficiency percentage above or equal to 80% and the drug release percentage at 24th h approximately between 20 and 25% were determined as constants in the DoE approach. Among the CuB-encapsulated hybrid nano-sized particles which were designed through the 3^2 factorial design in this research, LP5-coded formulation was selected as the optimum formulation due to having specified dependent variable limit values with this configuration. "*d*" value of the LP5-coded formulation based on this determined response variables was obtained as 0.92 through the Design-Expert software. In order to evaluate the reliability of the design model developed in this research, Bias % or Error % calculation was utilized by comparing the actual and predicted response variables of the optimum formulation. Bias % values of the predicted and actual values of the optimum formulation were calculated using the following equation:

$$\text{Bias } \% = (|\text{Predicted value} - \text{Actual value}|/\text{Predicted value}) \times 100$$

The Bias % value calculated for the *Q1* and *Q2* response variables was found as 4.36% and 0.10%, respectively. The fact that the Bias % values are less than 15% indicates that the predicted and actual response variables of optimum formulation are in good agreement [51].

Following the determination of the LP5-coded formulation as the optimum formulation, the further characterization studies of this hybrid nano-formulation were performed.

Thermal analysis of the optimum hybrid nano-sized particles

In this research, DSC analysis was also performed in the developed hybrid nano-sized drug carrier systems, as in all dosage forms, to determine the physical state of the CuB in the polymeric core, the possible interactions of the CuB with the PLGA, the DSPE-PEG and the lecithin, and also the thermal behavior of the CuB, the polymeric core material and the lipid materials. DSC thermograms of pure CuB, the LP5-coded optimum hybrid system and the blank form of this optimized formulation are presented in Fig. 6. When the DSC thermogram of pure CuB was examined, it was observed that CuB gave a sharp endothermic peak at 178.99 °C indicating its crystalline structure. This result is consistent with a previous study by Jianbo et al. [7]. On the other hand, when the DSC thermogram of the optimum formulation was evaluated, it was detected that the endothermic peak of CuB disappeared. This situation was interpreted as the crystal structure of CuB was returned to amorphous nature within the polymeric core structure after production process. Similar thermograms have been obtained by many researchers from time to time by loading hydrophobic active substances into polymer or lipid-based carriers [52].

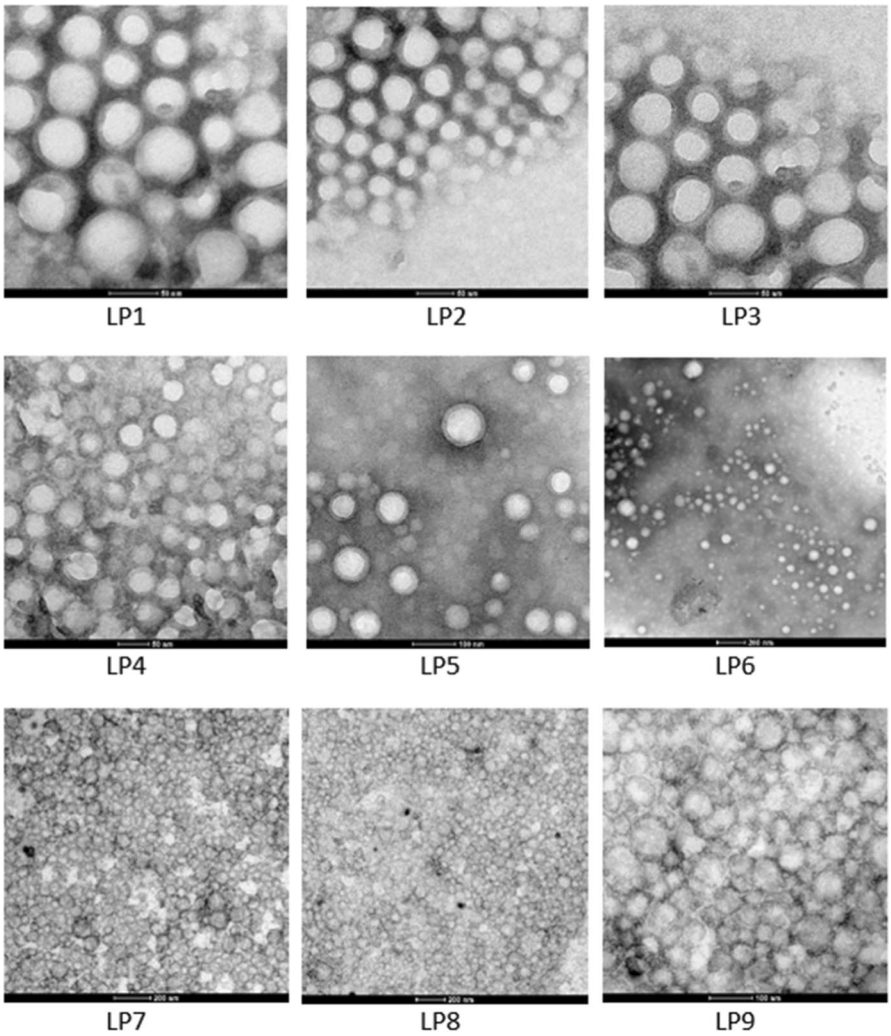

Fig. 4 TEM images of the CuB-encapsulated hybrid nano-sized particles

According to some researchers, the transformation of the crystalline structure of the active molecule to amorphous nature after entrapment of the active agent into the nano-systems like hybrid nanocarriers arose from the strong interactions between the lipid shell layers and the active molecule [53, 54]. When the thermograms of the blank form and the CuB-loaded nanocarriers were examined for peaks belonging to both lecithin and PEG-conjugated phospholipid, none of crystalline peaks were observed. This situation was thought to be due to the presence of amorphous nature of the lipid-based excipients. On the other hand, the peaks observed at 49.10 °C in the thermogram of CuB-loaded optimum formulation and also 45.82 °C in the

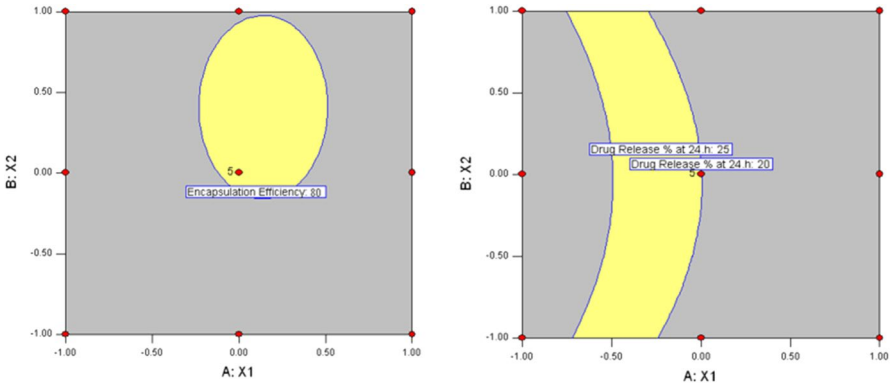

Fig. 5 Overlaid contour plots representing the applicable settings to achieve the desired values for both *Q1* (≥ 80%) and *Q2* (~ 20–25%)

thermogram of blank form of the hybrid system were based to the Tg (glass transition temperature) value of the PLGA. These Tg values of PLGA were consistent with our other researches mentioned above [31]. The results of DSC analysis demonstrated that CuB was in an amorphous nature in the polymeric core structure of the hybrid systems and no interaction was observed among CuB, PLGA, PEG-conjugated phospholipid and lecithin.

SAXS analysis of the hybrid nano-sized particles

The thicknesses of the shell lipid layers of the hybrid formulation at the center point of the design and also the formulations designed as a function of 34% of *X2* based on 0.1, 0.2 and 0.4 ratios of *X1* were calculated from the lipid transition layer width [31]. Table 4 shows the thickness values of the hybrid particles. This analysis demonstrated that lipid shell thickness of hybrid nano-sized particles increased significantly due to the increase in the PEG-conjugated phospholipid content in the hybrid systems ($p < 0.05$).

XPS analysis of the optimum hybrid nano-sized particles

The shell lipid layer consisting of the PEG-conjugated phospholipid was confirmed through the binding energies of the specific peaks. The peak observed at 133.6 mV was attributed to P2P envelope, which could only be ascribed to DSPE-PEG-COOH molecule on the surface of the particles according to the chemical composition of the optimum hybrid system. The band belonging to carboxyl group is C1s peak and consists of two components as C=O (289.2 mV) and C–OH bond (284.7 mV). These peaks and the binding energies of the PEG-conjugated phospholipid are consistent with a previous review by Chehimi et al. [55] (Fig. 7).

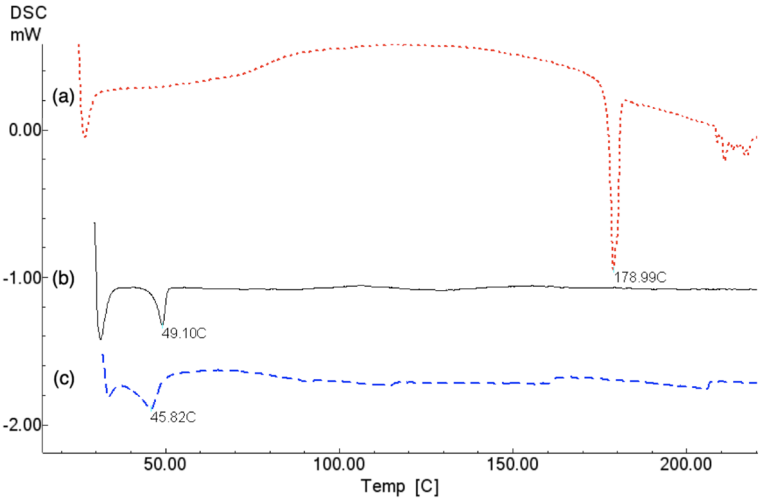

Fig. 6 DSC thermographs of **a** pure CuB, **b** selected CuB-encapsulated optimize hybrid nanocarrier and **c** optimized blank hybrid systems

Storage stability of the optimum hybrid nano-sized particles

Storage stability of the optimum hybrid nano-sized particles at different climatic conditions of 4 °C and 25 °C/60% RH was determined over 3- and 6-month periods in terms of the entrapment efficiency, particle size, PDI and zeta potential characteristics. Table 5 displays the results of the storage stability studies of the optimum formulation. When the 6-month stability data were evaluated statistically for the encapsulated CuB percentage into the hybrid system, it was determined that the hybrid system maintained the chemical structure of the active substance at both climatic conditions and no significant change was observed in terms of CuB amount loaded into the hybrid system ($p > 0.05$). When the mean particle size, PDI and surface charge of the optimum formulation which was stored at 4 °C were evaluated over a storage period of 6 months, no statistically significant variation was observed in any of the characteristic parameters ($p > 0.05$). On the other hand, particle size of the optimum formulation which was stored in 25 °C/60% RH was significantly increased from 113.8 to 425.7 nm in the first 3 months ($p < 0.05$), and degradations were also observed in the structure of the nanoparticles and particle size could not be determined at the end of the 6 months ($p < 0.05$). PDI values of hybrid nanosystems maintained at 25 °C/60% RH were significantly increased by the effect of time, temperature and humidity during the first 3-month period ($p < 0.05$). By the end of the 6 months, the PDI value was increased from 0.094 to 1.000 value and polydisperse particle size distribution occurred due to the formation of aggregations among the nanoparticles at the same climatic condition. Statistically significant decreases were observed in zeta potential values of nanoparticles which were stored at 25 °C/60% RH ($p < 0.05$). It is interpreted that the stability of the nanoparticle structure decreased significantly, especially in surface charge at this storage

Table 4 Thickness of shell lipid layer thickness of different hybrid nano-sized particles

Formulation codes	Shell lipid layer thickness (Armstrong, Å)
LP2	52.6
LP5	71.2
LP8	85.3

temperature and relative humidity value. As a result of the storage stability studies at the end of 6-month period, it was determined that the optimum hybrid nanoparticle formulation remained stable in terms of particle characteristics only at 4 °C when compared with 25 °C/60% RH.

Conclusion

In the present research, the core–shell-type hybrid nano-sized carriers of CuB, a BCS Class IV anticancer effective hydrophobic drug, were successfully produced through DoE approach. The influence of the critical formulation factors on the quality of final features of CuB-entrapped hybrid systems, i.e., entrapment efficiency and drug release percentage, was evaluated within the scope of this 3^2 factorial statistical design. The ANOVA results indicated that the ratios of PEG-conjugated phospholipid/biodegradable polymer and the total lipids/lecithin molar percentage improved the properties of the target variables of the CuB hybrid nano-sized carriers. The desirable function method was applied to select the optimum hybrid formulation of the design. The design data indicated that the optimum hybrid system

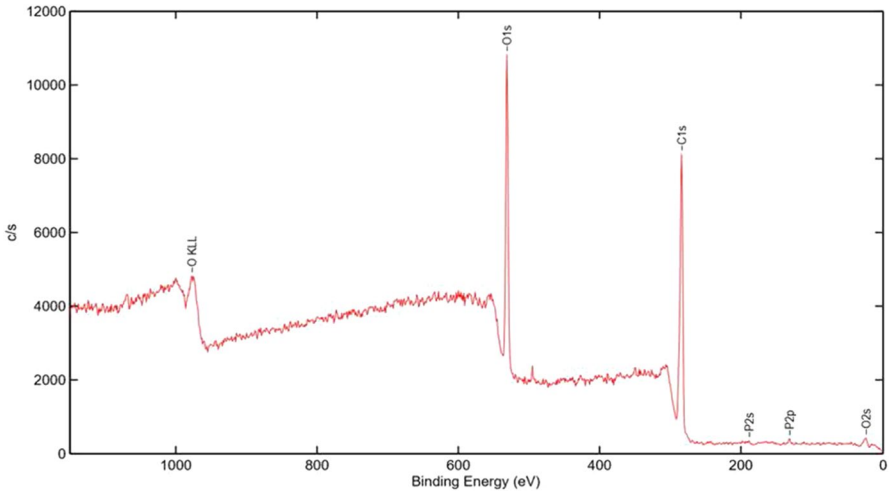

Fig. 7 XPS spectra of the optimum hybrid nano-sized particles

Table 5 Storage stability results of CuB-entrapped hybrid nanoparticles ($n = 3$)

Time	Storage conditions	Entrapment efficiency (%) ± SD	Particle size (nm) ± SD	PDI ± SD	Zeta potential (mV) ± SD
Initial		80.00 ± 4.97	113.8 ± 0.72	0.094 ± 0.02	− 36.6 ± 0.21
3 months	4 °C	78.65 ± 5.23	114.1 ± 1.71	0.100 ± 0.03	− 35.7 ± 2.12
	25 °C/60%RH	82.47 ± 7.08	425.7 ± 17.28	0.389 ± 0.45	− 23.6 ± 4.98
6 months	4 °C	81.27 ± 4.32	114.2 ± 2.85	0.113 ± 0.05	− 34.3 ± 3.27
	25 °C/60%RH	82.98 ± 6.29	–	1.000 ± 0.12	− 11.7 ± 7.49

SD standard deviation

was successfully designed with the *X1* value of 0.2 and *X2* value of 34% with the particle size of 113.8 nm, PDI value of 0.094, entrapment efficiency of 80% and surface charge of − 36.6 mV. The optimum lipid–polymer hybrid nano-sized carrier entrapped with CuB provided prolonged release of the active molecule (20.01%) during 24-h period. As a result of this study, an important design model has been developed in order to predict the statistical effectiveness of the critical formulation parameters which were effective on the final features of the hybrid nano-sized carriers optimized using DoE approach. In light of our results, further studies based on in vitro and in vivo experiments are planned to be performed to understand the potency of the CuB-entrapped optimized hybrid nanocarriers on cancer treatment.

Acknowledgements The authors would like to thank The Scientific and Technological Research Council of Turkey (TUBITAK) for their financial support to this research (Grant Number 117S131).

References

1. Kaushik U, Aeri V, Mi SR (2015) Cucurbitacins—an insight into medicinal leads from natüre. Pharmacognosy Rev 9(17):12–18
2. Li Y, Sheng Q, Zhang S, Lu Z, Guo J, Xu H, Deng Y (2010) Feasibility of percutaneous administration of cucurbitain B, an anticancer activity substances isolated from cucurbitaceae plants. Asian J Pharm Sci 5(4):152–160
3. Bakar F (2016) Cucurbitacin B enhances the anticancer effect of imatinib mesylate through inhibition of MMP-2 expression in MCF-7 and SW480 tumor cell lines. Anti Cancer Agents Med Chem 16(6):747–754
4. Chan KT, Meng FY, Li Q, Ho CY, Lam TS, To Y, Lee WH, Li M, Chu KH, Toh M (2010) Cucurbitacin B induces apoptosis and S phase cell cycle arrest in BEL-7402 human hepatocellular carcinoma cells and is effective via oral administration. Cancer Lett 294(1):118–124
5. Haritunians T, Gueller S, Zhang L, Badr R, Yin D, Xing H, Fung MC, Koeffler HP (2008) Cucurbitacin B induces differentiation, cell cycle arrest, and actin cytoskeletal alterations in myeloid leukemia cells. Leuk Res 32(9):1366–1373
6. Cheng L, Xu P, Shen B, Shen G, Li J, Qju L, Liu C, Yuan H, Han J (2015) Improve bile duct-targeted drug delivery and therapeutic efficacy for cholangiocarcinoma by cucurbitacin B loaded phospholipid complex modified with berberine hydrochloride. Int J Pharm 489:148–157
7. Jianbo G, Xue L, Hongdan Y, Zhaohui T, Xing T, Chenchen C, Jinghua X, Hui X (2013) The anti-melanoma efficiency of the intratumoral injection of cucurbitacin-loaded sustained-release carriers: a PLGA particle system. J Pharm Sci 102(8):2550–2563

8. Tang L, Fu L, Zhu Z, Yang Y, Sun B, Sun W, Zhang Z (2018) Modified mixed micelles with collagen peptides enhanced oral absorption of cucurbitacin B: preparation and evaluation. Drug Deliv 25(1):862–871
9. Ghadi R, Dand N (2017) BCS class IV drugs: highly notorious candidates for formulation development. J Control Release 248:71–95
10. Hu H, Liu D, Zhao X, Qiao M, Chen D (2013) Preparation, characterization, cellular uptake and evaluation in vivo of solid lipid nanoparticles loaded with cucurbitacin B. Drug Dev Ind Pharm 39:770–779
11. Wang W, Zhao X, Hu H, Chen D, Gu J, Deng Y, Sun J (2010) Galactosylated solid lipid nanoparticles with cucurbitacin B improves the liver targetability. Drug Deliv 17:114–122
12. Li Y, Han C, Li J, Quin L, Tang S (2014) Optimization of preparation of nanostructured lipid carriers loaded with cucurbitacin B by central composite design and response surface methodology. Chin J Pharm 45:1042–1045
13. Shen C, Li R, Shen B, Shen G, Wang L, Zheng J, Li X, Min H, Han J, Yuan H (2015) Influence of drug physicochemical characteristics on in vitro transdermal absorption of hydrophobic drug nanosuspensions. Drug Dev Ind Pharm 41:1997–2005
14. Lv Q, Li X, Li R, Shen B, Xu H, Shen C, Dai L, Han J, Yuan H (2014) Effective mucoadhesive water-soluble polymers for the solidification transformation of phospholipid-bile salts-mixed micelles. Pharmazie 69:792–798
15. Lv Q, Li X, Li R, Shen B, Xu H, Shen C, Dai L, Bai J, Yuan H, Han J (2014) Application of spray granulation for conversion of mixed phospholipid-bile salt micelles to dry powder: influence of drug hydrophobicity on nanoparticle reagglomeration. Int J Nanomed 9:505–515
16. Lv Q, Li X, Shen B, Dai L, Xu H, Shen C, Yuan H, Han J (2014) A solid phospholipid-bile salts-mixed micelles based on the fast dissolving oral films to improve the oral bioavailability of poorly water-soluble drug. J Nanopart Res 16:2455
17. Lv Q, Shen C, Li X, Shen B, Yu C, Xu P, Xu H, Han J, Yuan H (2015) Mucoadhesive buccal films containing phospholipid-bile salts-mixed micelles as an effective carrier for cucurbitacin B delivery. Drug Deliv 22:351–358
18. Bai X, Liu S, Yi L (2016) Cucurbitacin B nanometer liposome and preparation thereof. Patent CN 106137966
19. Zhang J, Chen J, Jiang X, Zhao H, Lei T, Zhang X (2016) A water-in-oil type nanoemulsion for significantly improving insoluble drug bioavailability, and preparation method thereof. Patent CN105977875
20. Zhang J, Lei T, Zhao H, Jiang X, Chen J, Zhang X (2016) An oil-in-water-type nano-emulsion capable of significantly increasing bioavailability of indissoluvable drugs, and preparation method thereof. Patent CN 10575212
21. Allen TM, Cullis PR (2013) Liposomal drug delivery systems: from concept to clinical applications. Adv Drug Deliv Rev 65:36–48
22. Lian T, Ho RJY (2001) Trends and developments in liposome drug delivery systems. J Pharm Sci 90:667–680
23. Panyam J, Labhasetwar V (2003) Biodegradable nanoparticles for drug and gene delivery to cells and tissue. Adv Drug Deliv Rev 55:329–347
24. Esim O, Savaser A, Kurbanoglu S, Kose-Ozkan C, Ozkan SA, Ozkan Y (2017) Development of assay for determination of eletriptan hydrobromide in loaded PLGA nanoparticles. J Pharm Biomed Anal 142:74–83
25. Hascicek C, Sengel-Turk CT, Gumustas M, Ozkan SA, Bakar F, Das-Evcimen N, Savaser A, Ozkan Y (2017) Fulvestrant-loaded polymer-based nanoparticles for local drug delivery: preparation and in vitro characterization. J Drug Deliv Sci Technol 40:73–82
26. Thanki K, Gangwal RP, Sangamwar AT, Jain S (2013) Oral delivery of anticancer drugs: challenges and opportunities. J Control Release 170:15–40
27. Sengel-Turk CT, Hascicek C, Bakar F, Simsek E (2017) Comparative evaluation of nimesulide-loaded nanoparticles for anticancer activity against breast cancer cells. AAPS PharmSciTech 18(2):393–403
28. Pantze SF, Parmentier J, Hofhaus G, Fricker G (2014) Matrix liposomes: a solid liposomal formulation for oral administration. Eur J Lipid Sci Technol 116:1145–1154
29. Fan Y, Zhang Q (2013) Development of liposomal formulations: from concept to clinical investigations. Asian J Pharm Sci 8:81–87
30. Mandal B, Bhattacharjee H, Mittal N, Sah H, Balabathula P, Thoma LA, Wood GC (2013) Core–shell-type lipid-polymer hybrid nanoparticles as a drug delivery platform. Nanomed 9:474–491

31. Sengel-Turk CT, Hascicek C (2017) Design of lipid-polymer hybrid nanoparticles for therapy of BPH: Part I. Formulation optimization using a design of experiment approach. J Drug Deliv Sci Technol 39:16–24
32. Yalcin TE, Ilbasmis-Tamer S, Takka S (2018) Development and characterization of gemcitabine hydrochloride loaded lipid polymer hybrid nanparticles (LPHNs) using central composite design. Int J Pharm 548:255–262
33. Mandal B, Mittal NK, Balabathula P, Thoma LA, Wood GC (2016) Development and in vitro evaluation of core-shell type lipid-polymer hybrid nanoparticles for the delivery of erlotinib in non-small cell lung cancer. Eur J Pharm Sci 81:162–171
34. Tahir N, Madni A, Balasubramanian V, Rehman M, Correia A, Kashif PM, Mäkilä E, Salonen J, Santos HA (2017) Development and optimization of methotrexate-loaded lipid-polymer hybrid nanoparticles for controlled drug delivery applications. Int J Pharm 533:156–168
35. Khorasani MT, Joorabloo A, Adeli H, Mansoori-Moghadam Z, Moghaddam A (2019) Design and optimization of process parameters of polyvinyl (alcohol)/chitosan/nano zinc oxide hydrogels as wound healing materials. Carbohydr Polym 207:542–554
36. Partovinia A, Vatankhah E (2019) Experimental investigation into size and sphericity of alginate microbeads produced by electrospraying technique: operational condition optimization. Carbohydr Polym 209:389–399
37. Turk CTS, Oz UC, Serim TM, Hascicek C (2014) Formulation and optimization of nonionic surfactants emulsified nimesulide-loaded PLGA-based nanoparticles by design of experiments. AAPS PharmSciTech 15(1):161–176
38. Sturm S, Stuppner H (2000) Analysis of cucurbitacins in medicinal plants by high-pressure liquid chromatography-mass spectrometry. Phytochem Anal 11(2):121–127
39. Bajcsik N, Pfab R, Pietsch J (2017) Simultaneous determination of cucurbitacin B, E, I and E-glucoside in plant material and body fluids by HPLC–MS. J Chromatogr B Analyt Technol Biomed Life Sci 1052:128–134
40. Shoaib M, Bahadur A, Saeed A, Saif ur Rahman M, Naseer MM (2018) Biocompatible, pH-responsive, and biodegradable polyurethanes as smart anti-cancer drug delivery carriers. React Funct Polym 127:153–160
41. Shoaib M, Saeed A, Saif Ur Rahman M, Naseer MM (2017) Mesoporous nano-bioglass designed for the release of imatinib and in vitro inhibitory effects on cancer cells. Mater Sci Eng C 77:725–730
42. Shoaib M, Saeed A, Akhtar J, Saif ur Rahman M, Ullahd A, Jurkschat K, Naseer MM (2017) Potassium-doped mesoporous bioactive glass: synthesis, characterization and evaluation of biomedical properties. Mater Sci Eng C 75:836–844
43. Shoaib M, Bahadur A, Saif ur Rahman M, Iqbal S, Arshad MI, Tahir MA, Mahmood T (2017) Sustained drug delivery of doxorubicin as a function of pH, releasing media, and NCO contents in polyurethane urea elastomers. J Drug Deliv Sci Technol 39:277–282
44. Shoaib M, Bahadur A, Iqbal S, Saif ur Rahman M, Ahmed S, Shabir G, Javaid MA (2017) Relationship of hard segment concentration in polyurethane-urea elastomers with mechanical, thermal and drug release properties. J Drug Deliv Sci Technol 37:88–96
45. Leng D, Thanki K, Fattal E, Foged C, Yang M (2018) Engineering of budesonide-loaded lipid-polymer hybrid nanoparticles using a quality-by-design approach. Int J Pharm 548(2):740–746
46. Aghamohammadi N, Aziz HB, Isa MH, Zinatizadeh AA (2007) Powdered activated carbon augmented activated sludge process for treatment of semi-aerobic landfill leachate using response surface methodology. Bioresour Technol 98(18):3570–3578
47. Kim CE, Lim SK, Kim JS (2012) In vivo antitumor effect of cromolyn in PEGylated liposomes for pancreatic cancer. J Control Release 157(2):190–195
48. Zhang L, Chan JM, Gu FX, Rhee JW, Wang AZ, Radovic-Moreno AF, Alexis F, Langer R, Farokhzad OC (2008) Self-assembled lipid-polymer hybrid nanoparticles: a robust drug delivery platform. ACS Nano 2:1696–1702
49. Pal S, Gauri SK (2018) A desirability functions-based approach for simultaneous optimization of quantitative and ordinal response variables in industrial processes. Int J Engineer Sci Technol 10(1):76–87
50. Yerlikaya F, Ozgen A, Vural I, Guven O, Karaagaoglu E, Khan MA, Capan Y (2013) Development and evaluation of paclitaxel nanoparticles using a quality-by-design approach. J Pharm Sci 102:3748–3761
51. Khan BC (2013) Bias in randomised factorial trials. Stat Med 32:4540–4549
52. Khuroo T, Verma D, Talegaonkar S, Padhi S, Panda AK, Iqbal Z (2014) Topotecan-tamoxifen douple PLGA polymeric nanoparticles: investigation of in vitro, in vivo and cellular uptake potential. Int J Pharm 473:384–394

53. Bikkad ML, Nathani AH, Mandlik SK, Shrotriya SN, Ranpise NS (2014) Halobetasol propionate-loaded solid lipid nanoparticles (SLN) for skin targeting by topical delivery. J Liposome Res 24:113–123
54. Shah B, Khunt D, Bhatt H, Misra M, Padh H (2015) Application of quality by design approach for intranasal delivery of rivastigmine loaded solid lipid nanoparticles: effect on formulation and characterization parameters. Eur J Pharm Sci 78:54–66
55. Chehimi MM, Djouani F, Benzarti K (2011) XPS studies of multiphase phase systems. In: Boudenne A, Ibos L, Candau Y, Thomas S (eds) Handbook of multiphase polymer systems. Wiley, New Delhi, pp 274–277